Research
A SCIENCE PARTNER JOURNAL

RESEARCH ARTICLE

Progesterone Enhances Niraparib Efficacy in Ovarian Cancer by Promoting Palmitoleic-Acid-Mediated Ferroptosis

Nayiyuan Wu[1,2†], Xiu Zhang[1,2†], Chao Fang[1,3†], Miaochen Zhu[1,2], Zhibin Wang[1,2], Lian Jian[1], Weili Tan[1], Ying Wang[1,2], He Li[1], Xuemeng Xu[1,2], Yujuan Zhou[1,2], Tang-Yuan Chu[1,4], Jing Wang[1,2*], and Qianjin Liao[1,2*]

[1]The Affiliated Cancer Hospital of Xiangya School of Medicine, Central South University/Hunan Key Laboratory of Cancer Metabolism, Hunan Cancer Hospital, Changsha 410078, Hunan, China. [2]Public Service Platform of Tumor Organoids Technology, Hunan Gynecological Tumor Clinical Research Center, Changsha 410013, Hunan, China. [3]Hunan Key Laboratory of the Research and Development of Novel Pharmaceutical Preparations, Changsha Medical University, Changsha 410219, Hunan, China. [4]Department of Obstetrics & Gynecology, Hualien Tzu Chi Hospital, Buddhist Tzu Chi Medical Foundation, Hualien 970, Taiwan, China.

*Address correspondence to: march-on@126.com; (Q.L.); wangjing0081@hnca.org.cn (J.W.)
†These authors contributed equally to this work.

Citation: Wu N, Zhang X, Fang C, Zhu M, Wang Z, Jian L, Tan W, Wang Y, Li H, Xu X, et al. Progesterone Enhances Niraparib Efficacy in Ovarian Cancer by Promoting Palmitoleic-Acid-Mediated Ferroptosis. *Research* 2024;7:Article 0371. https://doi.org/10.34133/research.0371

Submitted 12 December 2023
Accepted 10 April 2024
Published 24 May 2024

Poly (adenosine 5′-diphosphate-ribose) polymerase inhibitors (PARPi) are increasingly important in the treatment of ovarian cancer. However, more than 40% of *BRCA1/2*-deficient patients do not respond to PARPi, and *BRCA* wild-type cases do not show obvious benefit. In this study, we demonstrated that progesterone acted synergistically with niraparib in ovarian cancer cells by enhancing niraparib-mediated DNA damage and death regardless of *BRCA* status. This synergy was validated in an ovarian cancer organoid model and in vivo experiments. Furthermore, we found that progesterone enhances the activity of niraparib in ovarian cancer through inducing ferroptosis by up-regulating palmitoleic acid and causing mitochondrial damage. In clinical cohort, it was observed that progesterone prolonged the survival of patients with ovarian cancer receiving PARPi as second-line maintenance therapy, and high progesterone receptor expression combined with low glutathione peroxidase 4 (GPX4) expression predicted better efficacy of PARPi in patients with ovarian cancer. These findings not only offer new therapeutic strategies for PARPi poor response ovarian cancer but also provide potential molecular markers for predicting the PARPi efficacy.

Introduction

Epithelial ovarian cancer (EOC) generally presents at an advanced stage and is the most common cause of gynecological cancer death [1,2]. Poly (adenosine 5′-diphosphate-ribose) polymerase inhibitors (PARPi) have significantly improved maintenance therapy for recurrent ovarian cancer and are now approved as a first-line treatment for women with breast cancer susceptibility gene 1/2 (BRCA1/2) mutations [3–14]. However, only about 25% of patients with ovarian cancer have *BRCA* mutations [15,16]. Patients with BRCA wild-type ovarian cancer, especially those with homologous recombination deficiency (HRD)-negative tumors, do not benefit as much from PARPi [17–20], which limits their use in ovarian cancer therapy. In addition, except for the difference between BRCAness/PARPi sensitivity and non-BRCAness/PARPi resistance, EOCs (including type 1 and type 2 EOCs) are composed of distinct histological subtypes with unique genomic characteristics, resulting in inconsistent responses to PARPi [21–23]. Type 2 EOCs, including high-grade serous carcinoma (HGSC), carcinosarcoma, and undifferentiated carcinoma, are typically characterized by mutations in genes such as tumor protein P53 (*TP53*) and *BRCA1/2*. Type 1 EOCs, including several subtypes such as low-grade serous ovarian carcinoma, mucinous adenocarcinoma, endometrioid carcinoma, and clear cell carcinoma, are typically characterized by a specific pattern of mutations in genes such as *KRAS*, *BRAF*, and *PTEN*, which response poorly to PARPi. Therefore, improving the efficacy of PARPi in patients with ovarian cancer, especially non-BRCAness HGSC and type 1 EOC, is urgently required.

Niraparib, a PARPi, is approved for maintenance therapy in recurrent ovarian cancer, regardless of BRCA mutation status [13,24]. The PRIMA/PRIME and NOVA/NORA clinical studies demonstrated significant clinical efficacy of niraparib in patients with BRCA1/2 mutant ovarian cancer. However, its efficacy was reduced in patients with wild-type BRCA, particularly those with wild-type BRCA/HRD-negative status [13,24–26]. In addition, both the NOVA/NORA and PRIMA/PRIME studies found that niraparib causes adverse reactions in the digestive and

vascular systems of patients with ovarian cancer. In the NOVA study, 14.7% of patients discontinued the treatment, 68.9% interrupted the treatment, and 66.5% reduced drug dosage due to side effects; after 4 months, only 25% of patients continued the treatment at the initial dose. Consequently, the de-escalation of niraparib maintenance therapy while preserving clinical efficacy is crucial. Combination therapy with PARPi is urgently needed to address this challenge [27,28].

Progesterone (P4), a natural hormone produced by the ovary, is commonly used to treat well-differentiated EOC and endometrial cancer [29–34]. Epidemiological studies have shown that P4 can prevent the occurrence of ovarian cancer [35–40]. Our previous studies demonstrated that P4 could eliminate the precancerous cells in the fallopian tube either by inducing necroptosis through accelerating intracellular reactive oxygen species (ROS) and DNA damage [41] or by inducing pyroptosis through the paracrine inflammatory effect exerted by the adjacent fibroblasts [42]. Notably, intracellular ROS levels and DNA damage are closely associated with tumor cell sensitivity to PARPi [43,44], suggesting that P4 might improve the efficacy of niraparib in the treatment of ovarian cancer.

In this study, we investigated the therapeutic effect PARPi in combination with P4 in in vitro and in vivo cell models of type 1 and type 2 EOCs, as well as in organoid model of patients with HGSC. We demonstrated that P4 synergistically enhances the therapeutic activity of niraparib by inducing niraparib-mediated DNA damage in both type 1 and type 2 EOC cells regardless of the *BRCA*/HRD. We further demonstrated that P4 induced ferroptosis by promoting lipid oxidation and palmitoleic acid (POA) generation. Notably, P4 prolonged the survival of patients with ovarian cancer receiving PARPi as second-line maintenance therapy. In addition, P4 receptor (PR)-high/glutathione peroxidase 4 (GPX4)-low expression predicted better efficacy of PARPi and longer outcomes in patients with HGSC.

Results

P4 sensitizes ovarian cancer cells to niraparib by enhancing niraparib-mediated DNA damage and apoptosis

We selected 4 EOC cell lines in this study, including 2 type 2 HGSC cells—*BRCA* wild-type ($BRCA^{WT}$) OVCAR3 and *BRCA2*-mutated ($BRCA2^{Mut}$) PEO1—and 2 type 1 endometroid/clear cells—A2780 and SKOV3. PEO1 and OVCAR3 cells were treated with different concentrations of P4 plus niraparib (niraparib:P4 = 1:10, 1:6, 1:4, 1:2, 1:1, and 1:0.5) for 48 h. Synergetic effects [median effective dose (ED50) < 1] were observed for P4 plus niraparib at concentration ratios of niraparib:P4 between 1:4 and 1:0.5; the best combination indexes (CI) was found at niraparib:P4 = 1:1 in SKOV3, A2780, and PEO1 cells (Fig. 1A, Table 1, and Fig. S1A and B). Niraparib-induced growth inhibition (green line) was significantly enhanced by the P4 combined treatment (black line) in all 4 ovarian cancer cell lines tested (Fig. 1B).

Moreover, P4 sensitized cancer cells to niraparib reflected by lower IC_{50} values for niraparib in OVCAR3, SKOV3, A2780, and PEO1 cells (Fig. 1C and D). Further, compared with the *BRCA2*-mutated cell line PEO1, P4 significantly reduced IC_{50} in wild-type *BRCA* cell lines (OVCAR3, SKOV3, and A2780); the IC_{50} of OVCAR3 was reduced from 23.07 (20.79 to 25.60) μM to 5.903 (3.816 to 9.131) μM, the IC_{50} of SKOV3 was reduced from 23.39 (16.78 to 32.59) μM to 5.580 (2.671 to 11.65) μM, and the IC_{50} of A2780 was reduced from 33.22 (29.55 to 37.34) μM to 12.340 (7.978 to 19.08) μM, while the IC_{50} of PEO1 was reduced from 4.953 (4.414 to 5.558) μM to 2.410 (1.422 to 4.084) μM (Fig. 1D). Importantly, the ovarian cancer organoid model confirmed the synergistic effects of P4 and niraparib regardless of BRCA, and 10 HGSC cases were included. P4 combined with niraparib exerted satisfactory synergistic effects ($ED_{50} < 1$) and significantly inhibited cell viability in both niraparib-sensitive and -resistant cases (Fig. 1E and F and Table 2).

Clone formation, cell scratching, and Transwell assays were conducted on $BRCA^{WT}$ and $BRCA2^{Mut}$ ovarian cancer cells. Combined treatment with P4 and niraparib resulted in a substantial reduction in the number and dimensions of colonies, as well as a diminution in cellular invasion and metastatic potential (Fig. S1C to E) in both $BRCA^{WT}$ and $BRCA2^{Mut}$ cells compared with either niraparib or P4 monotherapy. Immunohistochemistry (IHC) and Western blot (WB) analyses demonstrated that the combined treatment with P4 and niraparib significantly elevated the levels of gamma histone family member X (γ-H2AX) compared to niraparib alone (Fig. 2A and B). The unrepaired double-strand break induced by this combinatorial approach triggered apoptosis, leading to a more pronounced apoptotic response compared to either agent administered independently in ovarian cancer cells (Fig. 2C). Collectively, these findings suggest that P4 potentiates the sensitivity of ovarian cancer cells to niraparib by exacerbating DNA double-strand break and inducing severe apoptosis.

P4 enhances the antitumor effect of niraparib prolonged survival in vivo

The peritoneal tumorigenesis mouse model and ovarian in situ tumorigenesis mouse model were established to confirm the synergistic effects of P4 and niraparib in vivo. In the ovarian in situ tumorigenesis model, after 15 d of administration of the drug, computed tomography (CT) images showed that ovarian tumor volumes were smaller in the P4 + niraparib combination group compared with the niraparib alone group. Representative images were shown in Fig. 3A and B. Ovarian tumor volumes were smaller in the combination group compared with the niraparib alone group in both the ovarian in situ (Fig. 3C and E) and peritoneal (Fig. 3D and F) tumorigenesis mouse models. In the mouse tumor tissue, IF showed higher γ-H2AX expression in the P4 + niraparib group compared with niraparib alone (Fig. 3G). In addition, the cell-proliferation-associated antigen Ki67 was suppressed, and apoptosis-related markers were induced in the P4 + niraparib group compared with the niraparib alone cohort (Fig. 3H). Survival experiments showed that the P4 + niraparib group significantly prolonged the survival time compared with niraparib alone in C57BL/6j mice (Fig. 3I). In vivo experiments confirmed the in vitro data, with P4 enhancing niraparib antitumor activity by inducing niraparib-mediated DNA damage and apoptosis in ovarian cancer cells.

P4 enhances the activity of niraparib in ovarian cancer by increasing fatty acid metabolism and POA production

To further explore the mechanisms of P4 promoting the inhibitory effect of niraparib on ovarian cancer, we performed metabolomics analysis, revealing that fatty acid oxidation metabolism were significantly enhanced in the niraparib plus P4 group

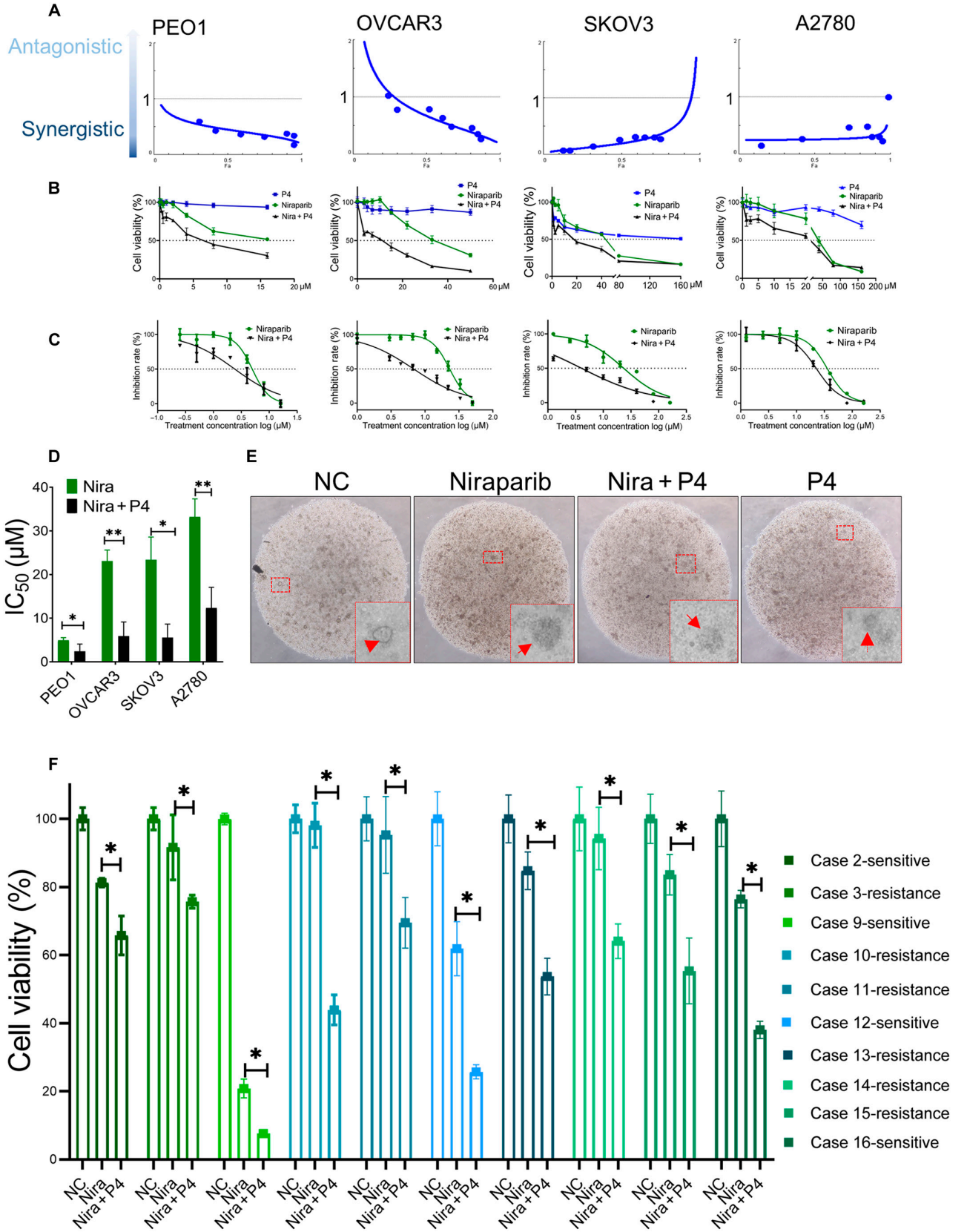

Fig. 1. P4 enhances the inhibitory effect of niraparib in ovarian cancer. (A) P4 plus niraparib combination treatment at a ratio of 1:1 in human *BRCA2*-mutated ovarian cancer cell line PEO1 and wild-type *BRCA* ovarian cancer cell lines OVCAR3, SKOV3, and A2780. (B) Cell counting kit-8 (CCK8) test cell viability in PEO1, OVCAR3, SKOV3, and A2780 cells treated with different concentration gradients of vehicle (NC), P4 (blue line), niraparib (green line), and P4 plus niraparib (black line) for 48 h. (C and D) half inhibitory concentration (IC_{50}) of PEO1, OVCAR3, SKOV3, and A2780 cells. (E) Representative images of ovarian cancer organoid tissues after the above treatment with vehicle, niraparib, P4 plus niraparib, or P4 for 5 d, acquired by light microscopy. (F) Cell viabilities in 10 ovarian cancer organoid tissue cases were tested after treatment with vehicle, niraparib, P4 plus niraparib or P4 for 5 d. $^{*}P < 0.05$; $^{**}P < 0.01$.

Table 1. Synergistic effect of P4 plus niraparib at different ratios

Ratio (niraparib:P4)	1:10	1:6	1:4	1:2	1:1	1:0.5
PEO1 CI (ED_{50})	1.02	0.92	0.91	0.45	0.38	0.45
OVCAR3 CI (ED_{50})	1.26	1.34	0.56	0.33	0.45	0.01
SKOV3 CI (ED_{50})	–	–	–	0.21	0.19	0.34
A2780 CI (ED_{50})	–	–	–	0.53	0.25	0.41

$0.9 \leq CI \leq 1.1$, the combination of the 2 drugs has superposition effect; $0.8 \leq CI < 0.9$, the combination of the 2 drugs has slight synergistic effect; $0.6 \leq CI < 0.8$, the combination of the 2 drugs has moderate synergistic effect; $0.4 \leq CI < 0.6$, the combination of the 2 drugs has satisfied synergistic effect; $0.2 \leq CI < 0.4$, the combination of the 2 drugs has great synergistic effect.

Table 2. Synergistic effect of niraparib plus P4 in organoid tissue

Case	CI (ED_{50})	Platinum sensitivity	Niraparib sensitivity	HRD status	BRCA status
Case 2	0.55	–	Sensitive	–	–
Case 3	0.73	Sensitive	Resistance	–	BRCA2 mutation
Case 9	1.02	Resistance	Sensitive	Positive	Wild
Case 10	0.61	Resistance	Resistance	Positive	Wild
Case 11	0.65	Sensitive	Resistance	–	–
Case 12	0.54	Sensitive	Sensitive	–	–
Case 13	0.78	Resistance	Resistance	–	Wild
Case 14	0.72	Resistance	Resistance	–	Wild
Case 15	0.68	Sensitive	Resistance	–	–
Case 16	0.47	Sensitive	Sensitive	Positive	BRCA1 mutation

$0.9 \leq CI \leq 1.1$, the combination of the 2 drugs has superposition effect; $0.8 \leq CI < 0.9$, the combination of the 2 drugs has slight synergistic effect; $0.6 \leq CI < 0.8$, the combination of the 2 drugs has moderate synergistic effect; $0.4 \leq CI < 0.6$, the combination of the 2 drugs has satisfied synergistic effect

compared with niraparib treatment alone (Fig. 4A and B). Quantitative metabolomics also demonstrated that production of POA and myristoleic acid (MA) was increased in the P4 plus niraparib group compared with the niraparib alone group (Fig. 4C). The CCK8 assay showed that POA, not MA, enhanced the inhibitory effect of niraparib in ovarian cancer cells (Fig. 4D). POA enhanced niraparib's antitumor activity by inducing niraparib-mediated DNA damage, and combined treatment with POA and niraparib significantly increased the levels of γ-H2AX (Fig. 4E and F).

To determine how P4 up-regulates POA in ovarian cancer cells, we performed transcriptomic sequencing of OVCAR3 cells. Results showed that the lipid metabolism signaling pathway was significantly enhanced in the combination therapy group (Fig. S2A), and multiple fatty-acid-metabolism-related genes were significantly up-regulated (Fig. S2B). To confirm the RNA sequencing results, we selected 10 significantly up-regulated genes involved in fatty acid metabolism (*SCD*, *FASN*, *DHCR7*, *MVD*, *ETV4*, *PER1*, *ACSS2*, *INSIG1*, *PSCK9*, and *FDFT1*) and analyzed those by quantitative real-time polymerase chain reaction (PCR) in OVCAR3, SKOV3, A2780, and PEO1 cells (Fig. S2C and Table S1). Treatment with P4 combined with niraparib significantly increased the expression of stearoyl-coenzyme A desaturase 1 (SCD1) compared with niraparib alone in ovarian cell lines (Fig. S2C and D). SCD1 inhibitors rescued the inhibitory effect of P4 plus niraparib on ovarian cancer cells (Fig. S2E). SCD1 was the rate-limiting enzyme required for the production of monounsaturated fatty acids from saturated fatty acids, such as converting palmitic acid (16) to POA (16, 1) [45,46]. This suggests that P4 up-regulates fatty acid metabolism and POA production by the expression of up-regulating fatty-acid-metabolism-related genes (SCD1, etc.).

How P4 and niraparib combination up-regulates SCD1 was further explored. We predicted the transcription factors of the *SCD* promoter via http://genome.ucsc.edu/. It was shown that *SCD* promoter could be bound by PR. In addition, PR

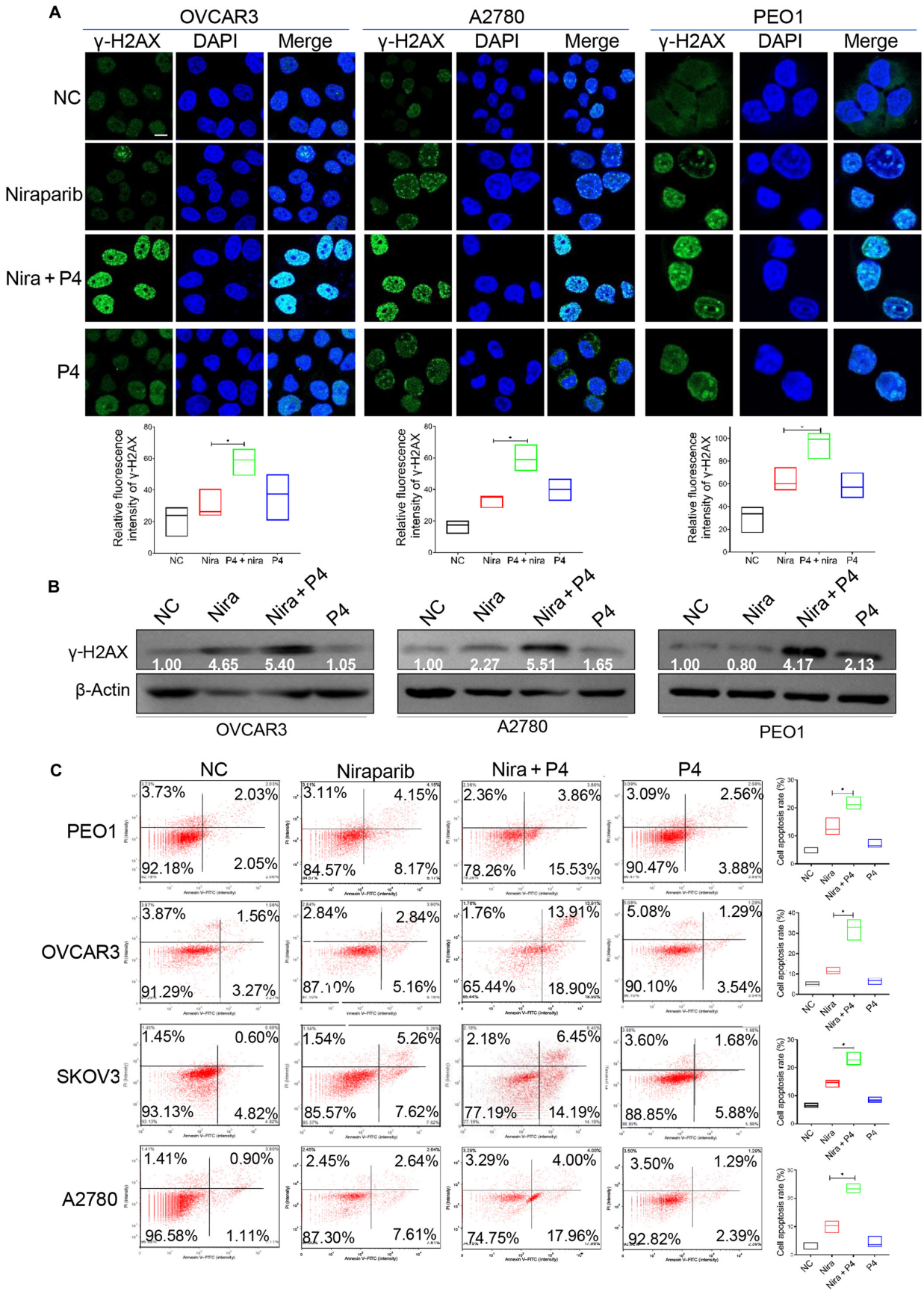

Fig. 2. P4 enhances the sensitivity of ovarian cancer cells to niraparib by inducing DNA damage and apoptosis. Ovarian cancer cells were treated with vehicle (NC), niraparib, P4 (10 μM) plus niraparib (10 μM), or P4 (10 μM) for 24 h, and IF (A) and WB (B) were performed to assess γ-H2AX expression. (C) Flow cytometry test cell death rate. The data in the graph represent annexin-V-positive cells. $^*P < 0.05$. Scale bar, 10 μM. FITC, fluorescein isothiocyanate.

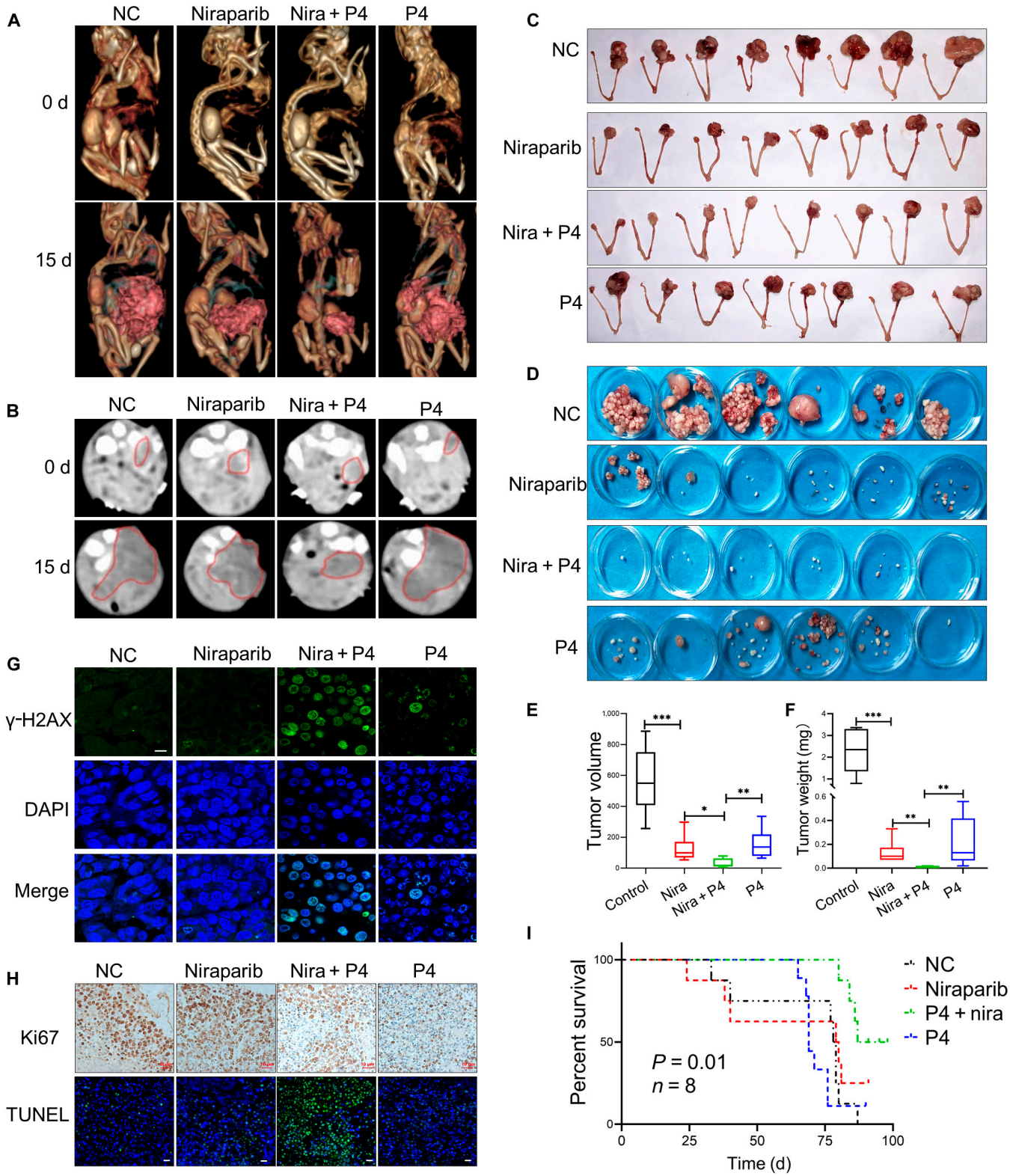

Fig. 3. P4 enhances the efficacy of niraparib in ovarian cancer in vivo. Representative 3-dimensional CT images (A) and CT scans (B) of ovarian in situ tumorigenesis mice before treatment (0 d) and 15 d after drug administration. (C and E) Ovarian in situ tumorigenesis mice and (D and F) intraperitoneal tumorigenesis mice treated with vehicle, niraparib (50 mg/kg), P4 plus niraparib (P4 at 5 mg/kg and niraparib at 50 mg/kg), or P4 (5 mg/kg); mice were sacrificed after 28 d of drug administration, and tumor sizes and weights were obtained. (G) Immunofluorescence (IF) test γ-H2AX expression in mouse tumor tissue samples; (H) IHC of the cell-proliferation-associated antigen Ki67 and the terminal-deoxynucleotidyl-transferase-mediated deoxyuridine triphosphate nick end labeling (TUNEL) test for apoptosis-related markers in the mouse tumor tissue. (I) Kaplan–Meier survival analysis of the survival of C57BL/6 mice in 4 different treatment groups ($n = 8$). $^*P < 0.05$; $^{**}P < 0.01$, $^{***}P < 0.001$. Scale bars,10 μm.

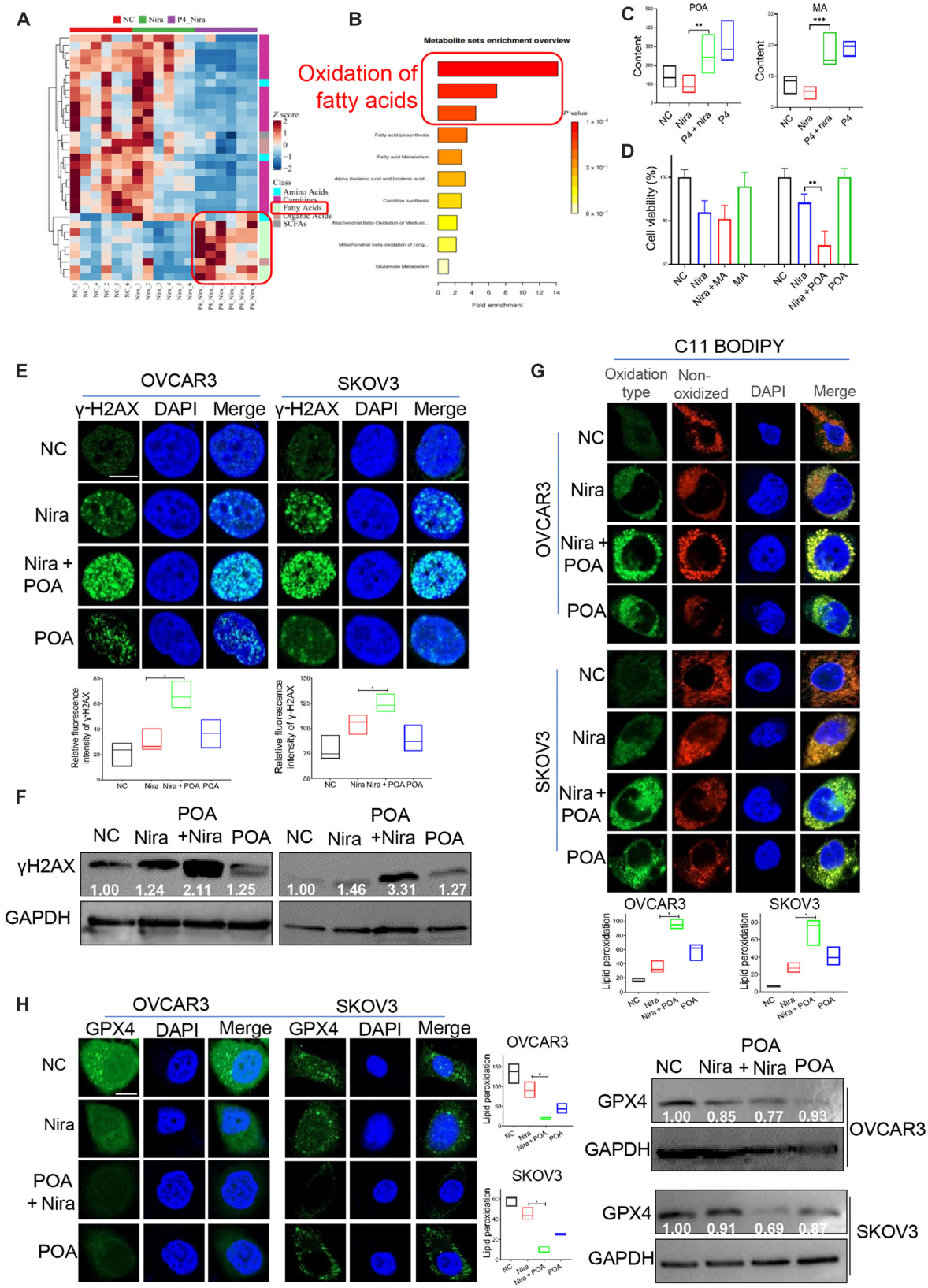

Fig. 4. P4 enhances the activity of niraparib by up-regulating fatty acid metabolism and POA production in ovarian cancer cells. (A) Metabolomics were performed in OVCAR3 cells after treated with vehicle (NC), niraparib, P4 plus niraparib, or P4 for 24 h; the *Z* score heatmap of the overall profile of metabolites. (B) Enrichment analysis results of metabolomics. (C) Detection of POA and MA in OVCAR3 cells after 24 h after the above treatment. (D) CCK8 assay tested the viability of OVCAR3 cells after 24 h of treatment with vehicle, niraparib, POA or MA + niraparib, POA, or MA. (E) IF and (F) WB were performed to assess the expression of γ-H2AX in OVCAR3 and SKOV3 cells after treatment with vehicle, niraparib (10 μM), POA (200 μM) + niraparib (10 μM), or POA (200 μM) for 24 h. (G) BODIPY 581/591 C11 staining was performed to quantify lipid peroxidation in OVCAR3 administered with the above treatment. (H) IF and WB were performed to assess GPX4 expression in OVCAR3 and SKOV3 cells administered with the above treatment. $^{*}P < 0.05$; $^{**}P < 0.01$; $^{***}P < 0.001$. Scale bar, 10 μm.

showed significant nuclear translocation in the P4 and niraparib combination group (Fig. S3A). Chromatin immunoprecipitation assay provides direct evidence for PR binding to SCD gene promoter in this study (Fig. S3B and C); the sterol regulatory element-binding protein 1 (SREBP1), which was identified as positive effectors of SCD transcription [47], was selected as positive control. This suggests that PR may act as a positive effector of SCD transcription.

P4 enhances the activity of niraparib in ovarian cancer by promoting ferroptosis

The oxidative metabolism of fatty acids, particularly lipid peroxidation, is closely related to ferroptosis [48,49]. In this study, BODIPY 581/591 C11 staining showed that niraparib plus POA markedly induced lipid peroxidation in ovarian cancer cells (Fig. 4G) and inhibited the expression of GPX4, which detoxified phospholipid peroxidation and protected the cells from ferroptosis (Fig. 4H). Similar results were observed in cells treated with P4 in combination with niraparib; treatment with P4 combined with niraparib significantly induced lipid peroxidation in the ovarian cancer cell lines. The potent ferroptosis inhibitor liproxstatin-1 (potent ferroptosis inhibitor) and RU486 (PR inhibitor) abolished the accumulation of lipid peroxides induced by niraparib plus P4 (Fig. 5A). Consistently, niraparib plus P4 significantly inhibited GPX4 expression (Fig. 5B and C and Fig. S4A), and liproxstatin-1 and RU486 rescued the inhibitory effect of P4 plus niraparib on GPX4 expression (Fig. 5B, D, and E). IF and flow cytometry revealed that Fe^{2+} amounts were significantly increased in the combination group compared with niraparib or P4 alone (Fig. 6A and Fig. S4B). P4 combined with niraparib induced severe mitochondrial damage (Fig. 6B and C) and increased ROS levels in OVCAR3 cells compared with niraparib alone (Fig. 6D and Fig. S4C). Mitochondria play important roles in triggering ferroptosis [50], and the generation of mitochondrial ROS is critical for lipid peroxidation and ferroptosis onset. Liproxstatin-1 and the ROS scavenger *N*-acetyl-L-cysteine (NAC) rescued the inhibitory effect of niraparib plus P4 on ovarian cancer cells (Fig. 6E). These data suggested that P4 increased the inhibitory effect of niraparib by promoting ferroptosis through fatty acid metabolism in ovarian cancer.

P4 enhances PARPi efficacy in ovarian cancer second-line maintenance therapy, and PR-high/GPX4-low expression was linked to better prognosis and higher PARPi sensitivity

To further explore the clinical application, we enrolled a total of 54 patients diagnosed with recurrence ovarian cancer who received PARPi as second-line maintenance therapy. Among them, 11 patients received P4 (medroxyprogesterone acetate) as a concomitant treatment for 1 to 3 months. The patient characteristics are displayed in Table 3. Kaplan–Meier survival analysis found that survival in the PARPi + P4 group was higher than that in the PARPi group: the median progression free interval (mPFI) was 53.07 months versus 24.73 months, the median progression free survival (mPFS) was 53.07 months versus 39.20 months, the median overall survival (mOS) was 62.30 months versus 52.73 months (Fig. 7A to C). IHC and IF showed the higher PR expression (Fig. 7D and E) and lower GPX4 expression (Fig. 7G and H) in PARPi-sensitive cases ($n = 9$) compared with PARPi-resistant cases ($n = 7$) (Table S2). High expression of PR (Fig. 7F) and low expression of GPX4 (Fig. 7I) were associated with longer survival.

Discussion

In this study, we found that P4 enhanced the efficiency of PARPis and prolonged survival in ovarian cancer. P4 acted synergistically with niraparib in ovarian cancer cells regardless of BRCA mutation status, and these synergistic effects were more pronounced in wild-type BRCA ovarian cancer cells. At the optimized mass ratios of 1:1, the addition of P4 to niraparib significantly inhibited cell viability and reduced IC_{50} by 0.5:1- to 4:1-fold compared with niraparib alone in ovarian cancer cell lines with or without *BRCA* mutation. The combination therapy significantly decreased colony formation and metastasis in both $BRCA^{WT}$ and $BRCA2^{Mut}$ cells compared with either niraparib or P4 alone. Notably, testing on the patient-derived organoids confirmed the synergistic effects with $ED_{50} < 1$ in both niraparib-sensitive and -resistant cases. The synergistic effect of P4 on niraparib is not limited to type 2 high-grade serous ovarian cancer cells. Two type 1 EOC cells, SKOV3 and A2780, are also sensitized by P4 for niraparib cytotoxicity. SKOV3 has characteristics of clear cell adenocarcinomas [51] with microsatellite instability and carries *ARID1A* and *MLH1* mutations. Molecular characterization of A2780 cells also showed a non-HGSC profile with *ARID1A*, *BRAF*, *PIK3CA*, and *PTEN* mutations, microsatellite instability, and wild-type TP53 [51–53].

P4, a low-toxicity therapeutic that targets various key pathways, has been used for over 80 years [54–56] and is crucial for cancer treatment and prevention [41,57]. In this study, niraparib plus P4 induced serious DNA damage and apoptosis in ovarian cancer cells and tumor tissues. It should be noted that DNA damage stress is an important determinant of PARPis' sensitivity. Niraparib is a highly selective inhibitor of PARP-1 and PARP-2, which are sensors of DNA damage that are most active during the S phase of the cell cycle [58–60]. These findings suggested that P4 may enhance the effects of PARPis by causing DNA damage and inducing cell death.

Ferroptosis is involved in the development and treatment response of various types of tumors [61–63]. In this study, P4 enhances the activity of niraparib in ovarian cancer by promoting ferroptosis through up-regulated lipid oxidation and POA production. Taken together, P4 enhances niraparib activity synergistically in ovarian cancer by promoting SCD1-mediated fatty acid oxidation and ferroptosis. EOC is characterized by high ROS stress and DNA damage loads with a saturation of DNA damage repair machineries, especially in the HRD high-grade serous carcinoma [64]. This saturated ROS/DNA damage load make ovarian cancer sensitive to the alkylating agents such as cisplatin that cause DNA replication catastrophe. The oversaturated DNA repair makes HRD ovarian cancer vulnerable to PARPis, which cause DNA repair catastrophe [65]. Adding P4 to PARPi deteriorates the ROS and DNA damage stress, overwhelms the DNA repair capacity, and kicks the cell into programed death.

Owing to the defective apoptosis due to p53 loss, overstressed HGSC cells undergo different nonapoptotic ways of death. In the precancerous state, P4 induces necroptosis of p53-mutated cells in the fallopian tube epithelium [41]. In therapeutic prevention model, P4 acts through the adjacent fibroblasts to deliver paracrine inflammatory stress to cancer cells, leading to pyroptosis [42]. The present study unveils the third way of cell death induced by P4, ferroptosis, by enhancing PARPi-induced ROS stress and DNA damage from SCD1-mediated lipid peroxidation.

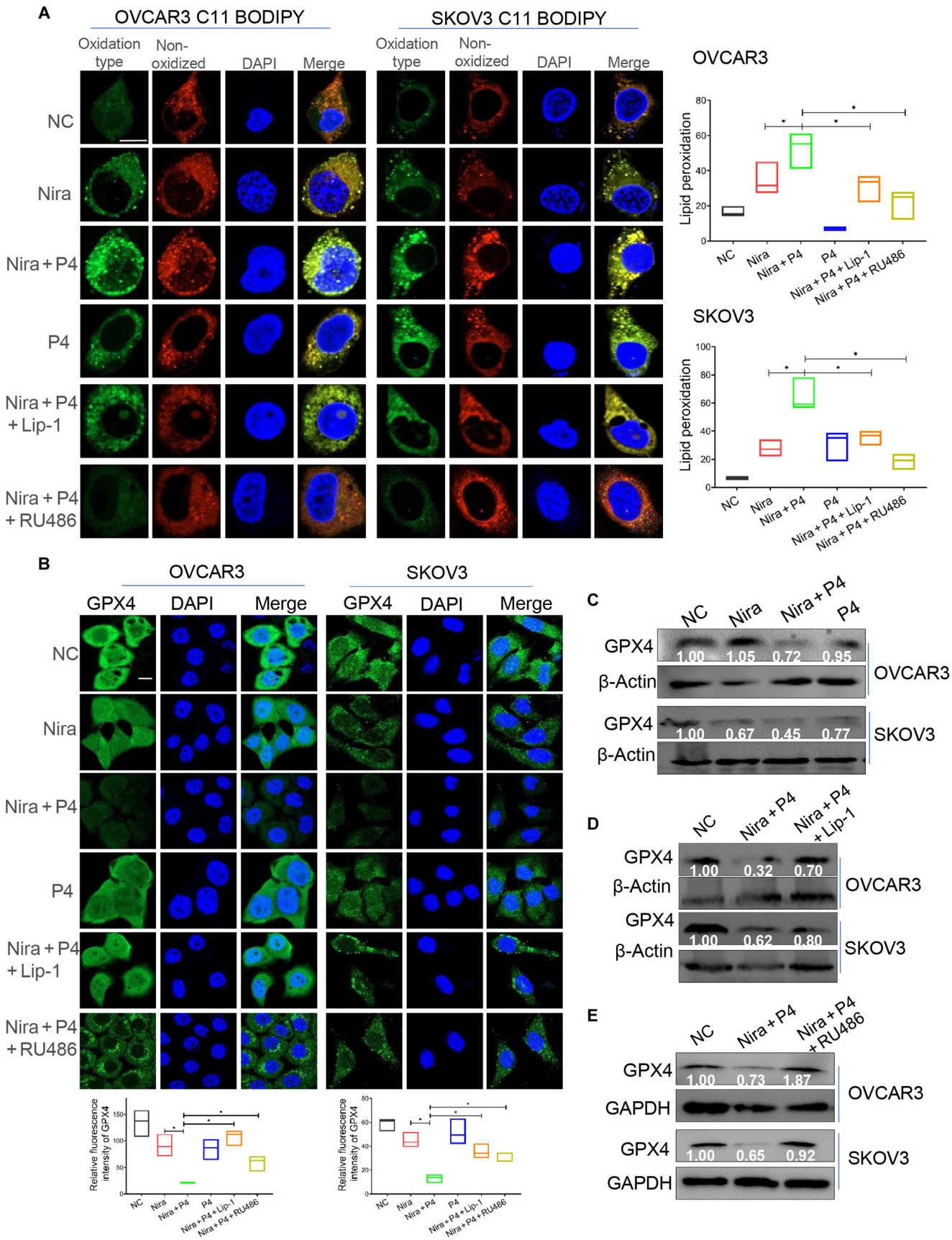

Fig. 5. P4 combined with niraparib promote lipid oxidation and GPX4 suppression. (A) BODIPY 581/591 C11 staining was performed to quantify lipid peroxidation in OVCAR3 and SKOV3 cells treated with vehicle (NC), P4 + niraparib, P4, P4 + niraparib + liproxstatin-1 (Lip-1) (1 μM), or P4 + niraparib + RU486 (5 μM) for 24 h. (B to E). IF and WB tested GPX4 expression in OVCAR3 and SKOV3 cells administered with the above treatments. *$P < 0.05$. Scale bars, 10 μm.

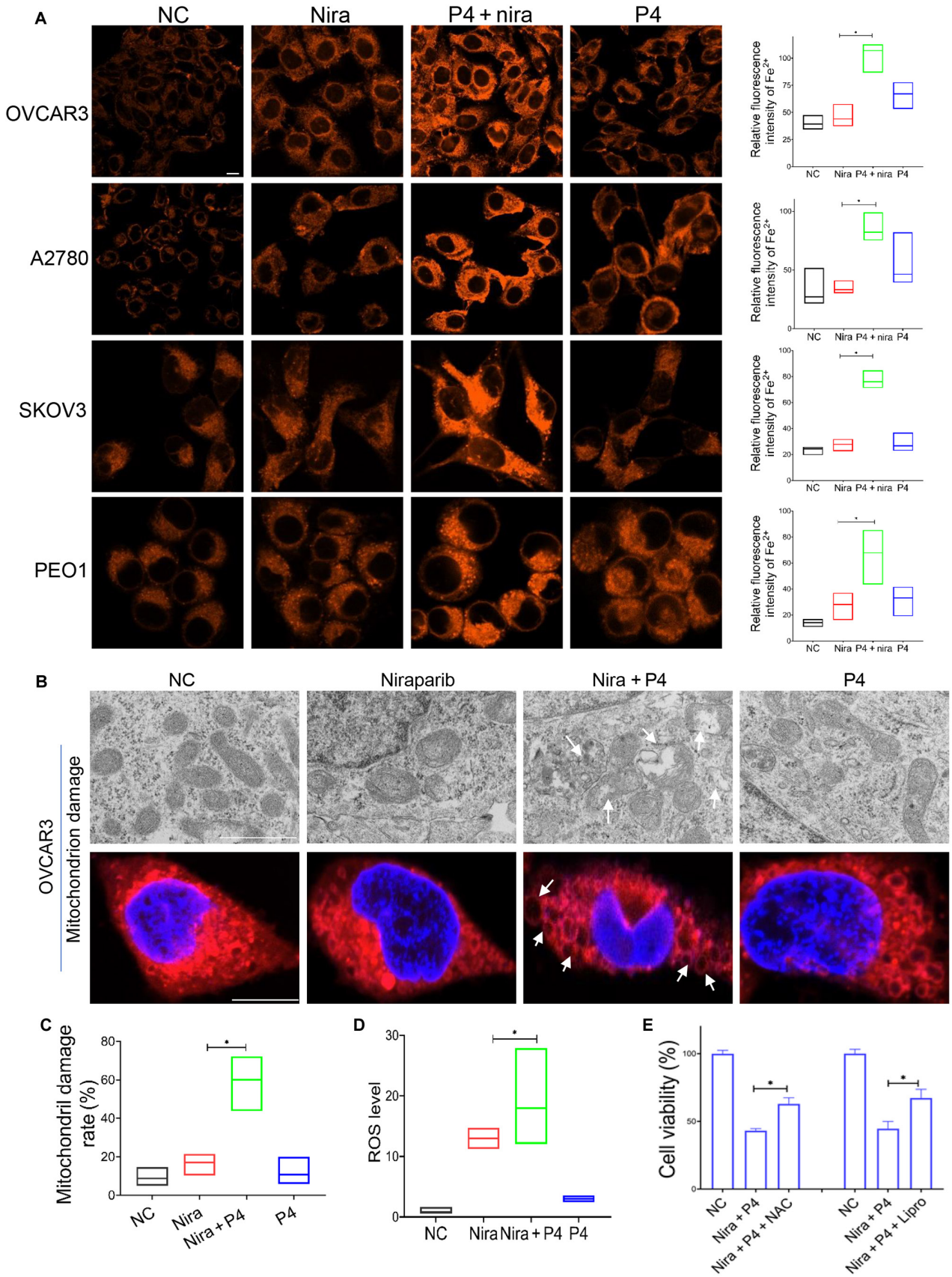

Fig. 6. P4 combined with niraparib promote ferroptosis in ovarian cancer cells. (A) IF determined Fe^{2+} levels in OVCAR3, A2780, SKOV3, and PEO1 cells treated with vehicle (NC), niraparib, P4 + niraparib, or P4 for 24 h. (B and C) Transmission electron microscope and IF observed mitochondrial damage of the OVCAR3 cells administered with the above treatments. (D) Flow cytometry test of ROS of OVCAR3 cells administered with the above treatments. (E) CCK8-tested ovarian OVCAR3 cell viability treated with vehicle, P4 + niraparib, P4 + niraparib + NAC, or liproxstatin-1. Scale bars, 10 μm (IF) and 1 μm (transmission electron microscope). *$P < 0.05$.

Table 3. Clinical characteristics of recurrence patients with ovarian cancer ($n = 54$)

Clinical characteristics	PARPi ($n = 43$)	PARPi + P4 ($n = 11$)	*P*
Age (years)	58.56 ± 7.79	56.64 ± 10.5	0.500
BMI (kg/m^2)	23.38 ± 3.24	22.44 ± 3.23	0.390
Total pregnancies	2.90 ± 1.57	2.90 ± 1.10	0.993
Childbirth	1.86 ± 0.87	1.30 ± 0.48	0.058
Abortion	1.07 ± 1.24	1.60 ± 1.27	0.232
Histological types			
HGSC	43	11	–
FIGO stages			
III	30	7	0.349
IV	5	3	
Unknown	8	1	
Gene mutations			
BRCA$^+$	2	1	0.465
BRCA$^-$	12	2	
Unknown	29	8	

BMI, body mass index; FIGO, International Federation of Gynecology and Obstetrics.

Materials and Methods

Cell culture

The human type 2 EOC cell lines (HGSC, PEO1 cells, BRCA2-mutated/OVCAR3 BRCA wild-type cells) and type 1 EOC cell lines (SKOV3/clear cell carcinoma, A2780/endometroid carcinoma) [66,67] as well as the mouse-derived ovarian cancer ID8 cell line were obtained from the Cancer Institute, Central South University. PEO1 and ID8 cells were cultured in DMEM high-glucose medium (Gibco, Life Technologies, Eugene, OR, USA) containing 10% FBS (Menlo Park, CA, USA), penicillin (100 μg/ml), and streptomycin (100 U/ml). OVCAR3, SKOV3, and A2780 cells were cultured in RPMI 1640 (Gibco, Life Technologies) containing 10% FBS, penicillin (100 μg/ml), and streptomycin (100 U/ml). All cell lines were cultured at 37 ˚C with 5% CO_2.

Cell Counting Kit-8 test

Ovarian cancer cells were seeded into 96-well plates at 5×10^3 per well, cultured for 24 h, and then treated with vehicle control, niraparib, P4 (P8783, Sigma-Aldrich) plus niraparib or P4 for 48 h. Then, 10 μl of the CCK8 reagent (KOO9-100, Zeta-Life) was added, and cells were incubated at 37 °C with 5% CO_2 in the dark for 2 h. Optical density was measured at 450 nm on a spectrophotometer. On the basis of the manufacturer's instructions, CIs at indicated fraction affected levels were calculated with the CompuSyn software by the Chou–Talalay method with nonconstant ratio combinations. The IC_{50} and CI values were calculated.

Colony formation assay

PEO1 and OVCAR3 cells were seeded into a 6-cm dish at 1×10^3 per dish and cultured for 24 h. Then, the cells were administered with niraparib (10 μM), P4 (10 μM), niraparib + P4, or vehicle control for 48 h. After formation, cell colonies were fixed with 95% alcohol for 30 min, stained with 1% crystal violet for 1.5 h, and washed with water. The colony formation rate was determined after drying.

Wound healing assay

PEO1, OVCAR3, SKOV3, and A2780 cells were seeded into 6-well plates at 5×10^5 per well. When the cells were ~90% confluent, using a sterile 10 μl pipette tip, the middle of the well was scratched. Next, the cells were administered with vehicle control niraparib (10 μM), P4 (10 μM), or niraparib + P4 for 48 h. Images were acquired at 0, 24, and 48 h after drug administration, and the healing area on the scratch was calculated with the ImageJ software.

Transwell migration assay

PEO1, OVCAR3, SKOV3, and A2780 cells were seeded into a Transwell chamber at 5×10^5 per well. After 6 h of culture, the cells were administered with niraparib (10 μM), P4 (10 μM), niraparib + P4, or vehicle control for 48 h. Then, the membranes with cells were fixed with 4% paraformaldehyde for 40 min and stained with 0.1% crystal violet solution for 20 min. Cells on the inner membrane were wiped with a cotton swab, and the chamber was washed with phosphate-buffered saline (PBS) to remove the excess staining solution. After drying, the chambers were imaged, and the numbers of migrated cells were determined.

Ovarian cancer organoid model

Cut fresh ovarian cancer tissue into 1- to 2-mm^3 fragments and dissociate at 37 °C for 1 to 2 h. Pass the dissociated cell suspension through a 70-mesh sieve; centrifuge and discard the supernatant. Mix the cell suspension with matrix adhesive, drop 30 μl of matrix adhesive in the center of the culture dish, place it in the incubator for solidification, and then add 250 μl of ovarian cancer organoid culture medium to ensure that the matrix adhesive is completely covered. Incubate in a 37 °C with 5% CO_2 incubator.

Flow cytometry

Cells seeded at 1×10^6 per well into 6-well plates were administered with niraparib (10 μM), P4 (10 μM), niraparib + P4, or vehicle control. Cells were collected by trypsinization and centrifugation. The annexin V/propidium iodide (PI) double-staining kit (Nanjing KeyGen Biotech Co. Ltd.) was used to determine the proportion of apoptotic cells by flow cytometry.

Mouse ovarian in situ tumorigenesis model and intraperitoneal tumorigenesis model experiment

Female C57BL/6 and BALB-nude mice at 6 to 7 weeks of age were purchased from SLA Laboratory. Female C57BL/6 mice were intraperitoneally injected with 1×10^5/ml of ID8 cells, and female BALB-nude mice were injected 2×10^5/ml of OVCAR3 cells into ovarian–tubal intrabursally or peritoneally. Then, the mice were divided into 4 groups ($n = 8$ per group), including vehicle, P4 (H33020828, Zhejiang Xianju Pharmaceutical; 5 mg/kg by intramuscular injection) [41,42] , niraparib (niraparib at 50 mg/kg by gavage) [68,69], and P4 plus niraparib (P4 at 5 mg/kg and niraparib at 50 mg/kg) groups. Therapy was started 10 d after tumor cells injection. Mice were continuously treated 3 times per week,

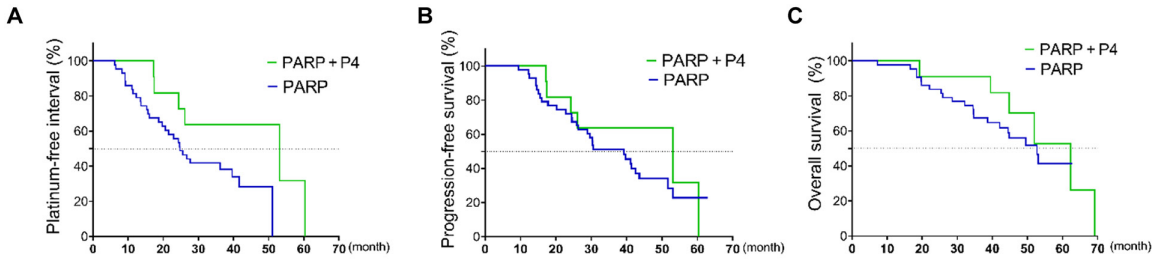

	PARPi (n = 43)	PARPi + P4 (n = 11)	HR (95% CI)	*P* value
mPFI	24.73 m	53.07 m	0.45 (0.22–0.93)	0.05
mPFS	39.20 m	53.07 m	0.74 (0.33–1.65)	0.46
mOS	52.73 m	62.30 m	0.76 (0.33–1.78)	0.39

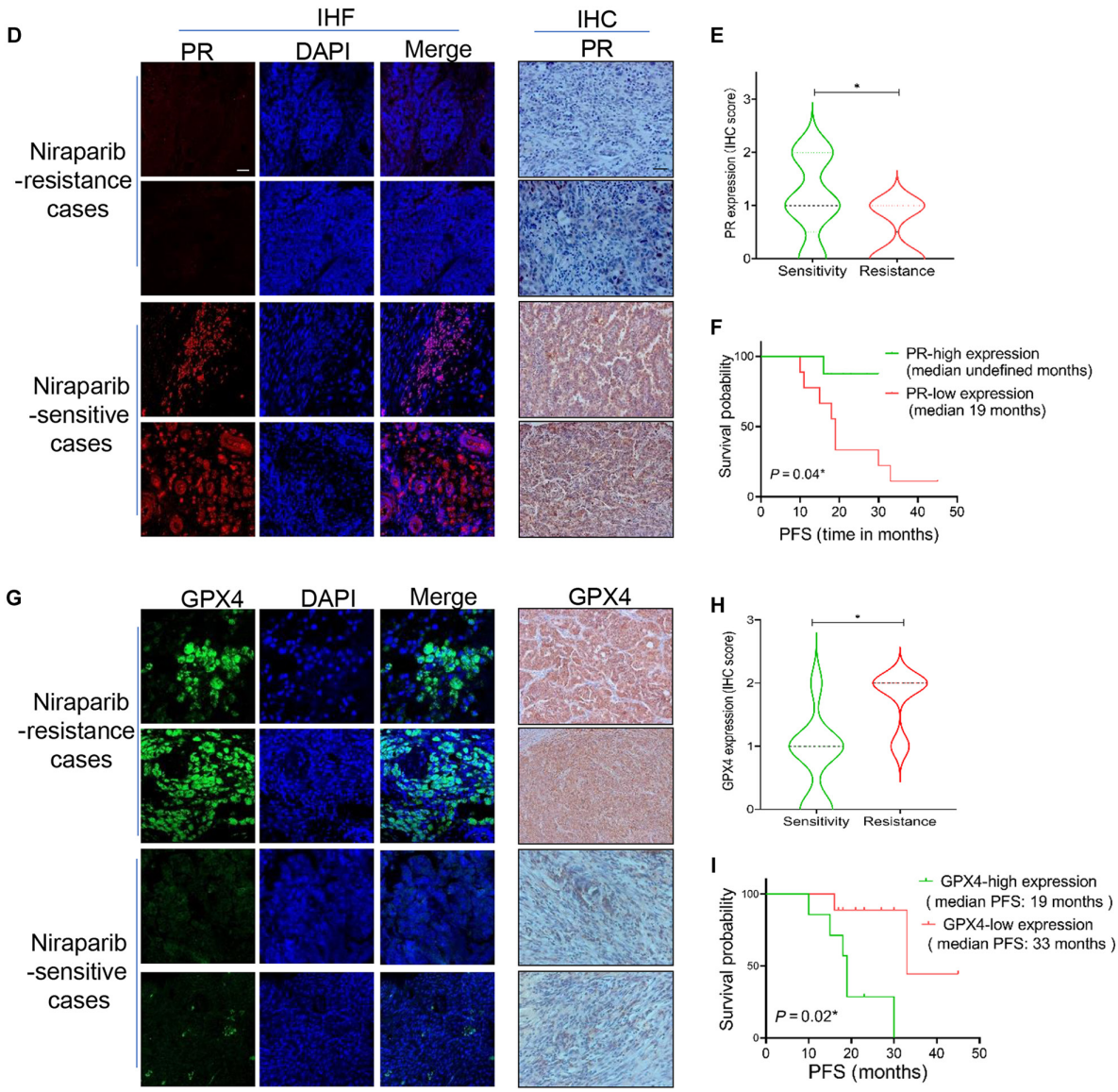

Fig. 7. P4 enhances PARPi efficacy in ovarian cancer second-line maintenance therapy, and PR-high/GPX4-low expression was linked to better prognosis and higher PARPi sensitivity. (A) PFI, (B) PFS, and (C) OS of patients with ovarian cancer received second-line maintenance therapy with or without concomitant P4 therapy. IF and IHC test the PR (D and E) and GPX4 (G and H) levels in PARPi-sensitive and -resistant ovarian cancer tissues. (F and I) PFS of patients with ovarian cancer administered with PARPi as maintenance therapy with different levels of PR/GPX4 expression. *$P < 0.05$. Scale bar, 10 μm. CI, confidence interval; HR, hazard ratio.

and animal body weights and ascites were observed. Mice were euthanized after 4 weeks of treatment, and tumor sizes, volumes, and tumor invasion and metastasis were recorded. Mouse tumors were fixed with 10% formalin, embedded in paraffin, and cut into 3-μm sections. Survival analysis of tumor-bearing mice after treatment with control, P4, niraparib, and P4 plus niraparib based on the methods mentioned above were also performed ($n = 8$ per group). The study protocol was approved by the Animal Ethics Committee of Hunan Cancer Hospital.

Immunofluorescene and immunohistochemistry

The tissue sections or adherent cells were washed with PBS after treatment, fixed with 4% paraformaldehyde, and permeabilized with 0.1% Triton X-100 in PBS. The samples were incubated with primary antibodies targeting γ-H2AX (ab81299, Abcam, Cambridge, MA, USA; 1:200), SCD1 (ab19862, Abcam; 1:200), Ki67 (ab16667, Abcam; 1:500), GPX4 (ab125066, Abcam; 1:200), and PR (ab2765, Abcam; 1:200), respectively, overnight at 4 °C. IF was followed by incubation with fluorescently labeled secondary antibodies (A11034, Invitrogen, Eugene, OR, USA; 1:1,000) in the dark for 1 h. Then, counterstaining was performed with 4′,6-diamidino-2-phenylindole (DAPI). Cell slides were analyzed by laser scanning confocal microscopy. IHC incubated with enhanced enzyme-labeled goat anti-mouse/rabbit immunoglobulin G (AWS0003a/AWS0002a, Abiowell; 1:1,000) at room temperature for 20 min, with subsequent staining with the DAB (3,3′-diaminobenzidine) kit (CWO125M, CWBIO).

Western blot

Proteins from ovarian cancer cells were extracted with radioimmunoprecipitation assay lysis buffer, and protein concentrations were determined with the BCA (bicinchoninic acid) kit. Each sample was loaded at 30 μg, subjected to SDS-polyacrylamide gel electrophoresis and transferred onto polyvinylidene difluoride membranes (Millipore, Burlington, MA, USA). Polyvinylidene difluoride membranes were blocked with 5% skimmed milk (Biosharp, Hefei, Anhui, China) for 2 h and incubated overnight at 4 °C with primary antibodies against β-actin (ab8227, Abcam; 1:1,000), glyceraldehyde-3-phosphate dehydrogenase (GAPDH; ab8245, Abcam; 1:1,000), γ-H2AX (ab81299, Abcam; 1:1,000), GPX4 (ab125066, Abcam; 1:1,000), and SCD1 (ab19862, Abcam; 1:1,000). Bound antibodies were then detected with horseradish-peroxidase-conjugated secondary antibodies (AWS0003a, Abiowell; 1:1,000). The ECL Western blotting substrate (Advansta, Munich, Germany) was used for visualization.

Metabonomics/metabolism

OVCAR3 cells were administered with vehicle, niraparib, niraparib plus P4, or P4 for 24 h, and then samples were thawed on ice bath to diminish sample degradation. Twenty microliters of plasma/serum was added to a 96-well plate. Then, the plate was transferred to the Eppendorf epMotion Workstation (Eppendorf Inc., Humburg, Germany). Ice-cold methanol (180 μl) with partial internal standards was automatically added to each sample and vortexed vigorously for 5 min. The plate was centrifuged at 4,000*g* for 30 min (Allegra X-15R, Beckman Coulter Inc., Indianapolis, IN, USA). Then, the plate was returned back to the workstation. Forty microliters of supernatant was transferred to a clean 96-well plate, and 20 μl of freshly prepared derivative reagents was added to each well. The plate was sealed, and the derivatization was carried out at 30 °C for 60 min. After derivatization, 420 μl of ice-cold acetonitrile was added to dilute the sample. Then, the plate was stored at −20 °C for 20 min and followed by 4,000*g* centrifugation at 4 °C for 30 min.

ROS test

OVCAR 3, SKOV3, A2780, and PEO1 cells were administered with vehicle, niraparib, niraparib plus P4, or P4 for 24 h; absorbing the culture medium and addition of serum-free medium and ROS (C6827, Invitrogen, USA) probe mixed reagent (10 μM), incubated at 37 °C for 30 min, and washed 3 times with serum-free medium. The collected cells were determined using by flow cytometry.

BODIPY 581/591 C11 test

OVCAR3, SKOV3, A2780, and PEO1 cells were implanted in laser confocal culture dishes; administered with vehicle, niraparib, niraparib plus P4, or P4 for 24 h, absorbing the culture medium; added BODIPY 581/591 C11 reagent (D3861, Invitrogen, USA; 10 μM); mixed culture medium; incubated at 37 °C for 30 min; absorbed working fluid; added serum-free culture medium after PBS washing; and then analyzed by confocal laser scanning microscopy.

Quantitative real-time polymerase chain reaction

Total RNA was extracted from OVCAR3, SKOV3, A2780, and PEO1 cells with TRIzol reagent (Ambion Inc., Austin, TX, USA). Total RNA was reverse-transcribed into complementary DNA with PrimeScript RT reagent kit with gDNA Eraser (TaKaRa Biotechnology, Dalian, China), following the manufacturer's instructions. TB Green Premix Ex Taq II (TaKaRa Biotechnology) was used for PCR on a LightCycle 480 II instrument. All primers were synthesized by Sangon Biotechnology Company (Shanghai, China) and are listed in Table S1. The relative mRNA expression was calculated by the $2^{-\Delta\Delta Ct}$.

Patient cohort

The retrospective cohort included 54 patients diagnosed with recurrent EOC who received PARPi as maintenance therapy between 2019 and 2021 at Hunan Cancer Hospital; among them, 11 people were taking P4 (megestrol acetate dispersible tablets, H20040001) a concomitant treatment for 1 to 3 months. The inclusion criteria are as follows: (a) platinum sensitivity; (b) the efficacy of primary treatment achieves partial or complete remission; and (c) PARPi was received as maintenance therapy more than 6 months. The exclusion criteria are as follows: (a) without platinum-based chemotherapy; (b) treated with other targeted drugs except PARPi; (c) clinical information missing; (d) missed follow-up. The study protocol was approved by the Institutional Review Board of Hunan Cancer Hospital.

Statistical analysis

Progression-free survival (PFS) was the time starting from patients' enrollment until tumor progression or death. Platinum-free interval (PFI) refers to the time from completion of the last platinum-containing chemotherapy course to recurrence. Overall survival (OS) refers to the time from patients' enrollment to death.All data were obtained from 3 independent replicates, and the results were expressed as means ± SD. Statistical analysis was performed with SPSS version 18.0 or GraphPad. Two-sample *t* test or nonparametric test was used to compare group pairs.

The chi-square test was used for categorical data. Kaplan–Meier analysis was performed to assess the prognosis of patients with ovarian cancer, and the log-rank test was performed to compare survival. $P < 0.05$ was considered statistically significant.

Acknowledgments

We would like to thank J. Yu of Zai laboratory and FigDraw.
Funding: This work was supported by the National Natural Science Foundation of China (82003050 and 82173142), Hunan Provincial Natural Science Foundation (2023JJ30375 and 2023JJ60016), Hunan Cancer Hospital Climb Plan (2023NSFC-A004 and 2023NSFC-A003), and Changsha Science and Technology Board (kh2201054), Hunan Provincial Health Commission (B2023047708).
Author contributions: N.W. contributed to molecular experiments and manuscript writing. C.F., X.Z., and M.Z. contributed to sample collection and animal experiments. C.F., L.J., W.T., and X.X. contributed to mouse CT photography and analysis. Z.W., Y.W., Y.Z., and H.L. contributed to technical support for data analysis and study conception. Q.L., T-Y.C., and J.W. contributed to study conception and design and the final approval of the submitted version.
Competing interests: The authors declare that they have no competing interests.

Data Availability

Data will be made available on request.

Supplementary Materials

Figs. S1 to S4
Tables S1 and S2

References

1. Siegel RL, Giaquinto AN, Jemal A. Cancer statistics, 2024. *CA Cancer J Clin*. 2024;74(1):12–49.
2. Torre LA, Trabert B, DeSantis CE, Miller KD, Samimi G, Runowicz CD, Gaudet MM, Jemal A, Siegel RL. Ovarian cancer statistics, 2018. *CA Cancer J Clin*. 2018;68(4):284–296.
3. Groelly FJ, Fawkes M, Dagg RA, Blackford AN, Tarsounas M. Targeting DNA damage response pathways in cancer. *Nat Rev Cancer*. 2023;23(2):78–94.
4. da Costa A, Chowdhury D, Shapiro GI, D'Andrea AD, Konstantinopoulos PA. Targeting replication stress in cancer therapy. *Nat Rev Drug Discov*. 2023;22(1):38–58.
5. Huang D, Kraus WL. The expanding universe of PARP1-mediated molecular and therapeutic mechanisms. *Mol Cell*. 2022;82(12):2315–2334.
6. Dao F-Y, Lv H, Fullwood MJ, Lin H. Accurate identification of DNA replication origin by fusing epigenomics and chromatin interaction information. *Research*. 2022;2022:9780293.
7. Concannon K, Morris BB, Gay CM, Byers LA. Combining targeted DNA repair inhibition and immune-oncology approaches for enhanced tumor control. *Mol Cell*. 2023;83(5):660–680.
8. Garg V, Oza AM. Treatment of ovarian cancer beyond PARP inhibition: Current and future options. *Drugs*. 2023;83(15):1365–1385.
9. DiSilvestro P, Banerjee S, Colombo N, Scambia G, Kim BG, Oaknin A, Friedlander M, Lisyanskaya A, Floquet A, Leary A, et al. Overall survival with maintenance olaparib at a 7-year follow-up in patients with newly diagnosed advanced ovarian cancer and a BRCA mutation: The SOLO1/GOG 3004 trial. *J Clin Oncol*. 2023;41(3):609–617.
10. Banerjee S, Moore KN, Colombo N, Scambia G, Kim BG, Oaknin A, Friedlander M, Lisyanskaya A, Floquet A, Leary A, et al. Maintenance olaparib for patients with newly diagnosed advanced ovarian cancer and a BRCA mutation (SOLO1/GOG 3004): 5-year follow-up of a randomised, double-blind, placebo-controlled, phase 3 trial. *Lancet Oncol*. 2021;22(12):1721–1731.
11. DiSilvestro P, Colombo N, Scambia G, Kim BG, Oaknin A, Friedlander M, Lisyanskaya A, Floquet A, Leary A, Sonke GS, et al. Efficacy of maintenance olaparib for patients with newly diagnosed advanced ovarian cancer with a BRCA mutation: Subgroup analysis findings from the SOLO1 trial. *J Clin Oncol*. 2020;38(30):3528–3537.
12. Moore K, Colombo N, Scambia G, Kim BG, Oaknin A, Friedlander M, Lisyanskaya A, Floquet A, Leary A, Sonke GS, et al. Maintenance olaparib in patients with newly diagnosed advanced ovarian cancer. *N Engl J Med*. 2018;379(26):2495–2505.
13. González-Martín A, Pothuri B, Vergote I, DePont Christensen R, Graybill W, Mirza MR, McCormick C, Lorusso D, Hoskins P, Freyer G, et al. Niraparib in patients with newly diagnosed advanced ovarian cancer. *N Engl J Med*. 2019;381(25):2391–2402.
14. Li N, Zhu J, Yin R, Wang J, Pan L, Kong B, Zheng H, Liu J, Wu X, Wang L, et al. Treatment with niraparib maintenance therapy in patients with newly diagnosed advanced ovarian cancer: A phase 3 randomized clinical trial. *JAMA Oncol*. 2023;9(9):1230–1237.
15. Norquist BM, Harrell MI, Brady MF, Walsh T, Lee MK, Gulsuner S, Bernards SS, Casadei S, Yi Q, Burger RA, et al. Inherited mutations in women with ovarian carcinoma. *JAMA Oncol*. 2016;2(4):482–490.
16. Pillay N, Tighe A, Nelson L, Littler S, Coulson-Gilmer C, Bah N, Golder A, Bakker B, Spierings DCJ, James DI, et al. DNA replication vulnerabilities render ovarian cancer cells sensitive to poly(ADP-ribose) glycohydrolase inhibitors. *Cancer Cell*. 2019;35(3):519–533.e8.
17. Mateo J, Lord CJ, Serra V, Tutt A, Balmaña J, Castroviejo-Bermejo M, Cruz C, Oaknin A, Kaye SB, de Bono JS. A decade of clinical development of PARP inhibitors in perspective. *Ann Oncol*. 2019;30(9):1437–1447.
18. Fugger K, Hewitt G, West SC, Boulton SJ. Tackling PARP inhibitor resistance. *Trends Cancer*. 2021;7(12):1102–1118.
19. Murai J, Pommier Y. BRCAness, homologous recombination deficiencies, and synthetic lethality. *Cancer Res*. 2023;83(8):1173–1174.
20. Incorvaia L, Perez A, Marchetti C, Brando C, Gristina V, Cancelliere D, Pivetti A, Contino S, di Giovanni E, Barraco N, et al. Theranostic biomarkers and PARP-inhibitors effectiveness in patients with non-BRCA associated homologous recombination deficient tumors: Still looking through a dirty glass window? *Cancer Treat Rev*. 2023;121:102650.
21. Pavlik EJ, Smith C, Dennis TS, Harvey E, Huang B, Chen Q, Piecoro DW, Burgess BT, McDowell A, Gorski J, et al. Disease-specific survival of type I and type II epithelial ovarian cancers-stage challenges categorical assignments of indolence & aggressiveness. *Diagnostics*. 2020;10(2):56.

22. Nik NN, Vang R, Shih IM, Kurman RJ. Origin and pathogenesis of pelvic (ovarian, tubal, and primary peritoneal) serous carcinoma. *Annu Rev Pathol*. 2014;9:27–45.
23. Kurman RJ, Shih Ie M. The dualistic model of ovarian carcinogenesis: Revisited, revised, and expanded. *Am J Pathol*. 2016;186(4):733–747.
24. Mirza MR, Monk BJ, Herrstedt J, Oza AM, Mahner S, Redondo A, Fabbro M, Ledermann JA, Lorusso D, Vergote I, et al. Niraparib maintenance therapy in platinum-sensitive, recurrent ovarian cancer. *N Engl J Med*. 2016;375(22): 2154–2164.
25. Wu XH, Zhu JQ, Yin RT, Yang JX, Liu JH, Wang J, Wu LY, Liu ZL, Gao YN, Wang DB, et al. Niraparib maintenance therapy in patients with platinum-sensitive recurrent ovarian cancer using an individualized starting dose (NORA): A randomized, double-blind, placebo-controlled phase III trial(☆). *Ann Oncol*. 2021;32(4):512–521.
26. Li N, Zhu J, Yin R, Wang J, Pan L, Kong B, Zheng H, Liu J, Wu X, Wang L, et al. Treatment with niraparib maintenance therapy in patients with newly diagnosed advanced ovarian cancer: A phase 3 randomized clinical trial. *JAMA Oncol*. 2023;**9**(9):1230–1237.
27. Chu YY, Chen MK, Wei Y, Lee HH, Xia W, Wang YN, Yam C, Hsu JL, Wang HL, Chang WC, et al. Targeting the ALK-CDK9-Tyr19 kinase cascade sensitizes ovarian and breast tumors to PARP inhibition via destabilization of the P-TEFb complex. *Nat Cancer*. 2022;3(10):1211–1227.
28. Li J, Zhi X, Chen S, Shen X, Chen C, Yuan L, Guo J, Meng D, Chen M, Yao L. CDK9 inhibitor CDKI-73 is synergetic lethal with PARP inhibitor olaparib in BRCA1 wide-type ovarian cancer. *Am J Cancer Res*. 2020;10(4):1140–1155.
29. Ruiz MP, Huang Y, Hou JY, Tergas AI, Burke WM, Ananth CV, Neugut AI, Hershman DL, Wright JD. All-cause mortality in young women with endometrial cancer receiving progesterone therapy. *Am J Obstet Gynecol*. 2017;217(6):669.e1–669.e13.
30. Pyrzak A, Chen L, Kocherginsky M, Barber EL. Radiation and hormonal therapy for primary treatment of stage I endometrial cancer and long-term survival. *Gynecol Oncol*. 2020;158(2):331–338.
31. Greenwald ZR, Huang LN, Wissing MD, Franco EL, Gotlieb WH. Does hormonal therapy for fertility preservation affect the survival of young women with early-stage endometrial cancer? *Cancer*. 2017;123(9):1545–1554.
32. Park JY, Kim DY, Kim JH, Kim YM, Kim KR, Kim YT, Seong SJ, Kim TJ, Kim JW, Kim SM, et al. Long-term oncologic outcomes after fertility-sparing management using oral progestin for young women with endometrial cancer (KGOG 2002). *Eur J Cancer*. 2013;49(4):868–874.
33. Ho S-M. Estrogen, progesterone and epithelial ovarian cancer. *Reprod Biol Endocrinol*. 2003;1:73.
34. Mitra S, Lami MS, Ghosh A, Das R, Tallei TE, Fatimawali, Islam F, Dhama K, Begum MY, Aldahish A, et al. Hormonal therapy for gynecological cancers: How far has science progressed toward clinical applications? *Cancers*. 2022;14(3):759.
35. Lima MA, Silva SV, Jaeger RG, Freitas VM. Progesterone decreases ovarian cancer cells migration and invasion. *Steroids*. 2020;161:108680.
36. Collaborative Group on Epidemiological Studies of Ovarian Cancer, Beral V, Doll R, Hermon C, Peto R, Reeves G. Ovarian cancer and oral contraceptives: Collaborative reanalysis of data from 45 epidemiological studies including 23,257 women with ovarian cancer and 87,303 controls. *Lancet*. 2008;371(9609):303–314.
37. Huang T, Townsend MK, Wentzensen N, Trabert B, White E, Arslan AA, Weiderpass E, Buring JE, Clendenen TV, Giles GG, et al. Reproductive and hormonal factors and risk of ovarian cancer by tumor dominance: Results from the ovarian cancer cohort consortium (OC3). *Cancer Epidemiol Biomarkers Prev*. 2020;29(1):200–207.
38. Grandi G, Toss A, Cortesi L, Botticelli L, Volpe A, Cagnacci A. The association between endometriomas and ovarian cancer: Preventive effect of inhibiting ovulation and menstruation during reproductive life. *Biomed Res Int*. 2015;2015:751571.
39. Grimbizis GF, Tarlatzis BC. The use of hormonal contraception and its protective role against endometrial and ovarian cancer. *Best Pract Res Clin Obstet Gynaecol*. 2010;24(1):29–38.
40. Modan B, Hartge P, Hirsh-Yechezkel G, Chetrit A, Lubin F, Beller U, Ben-Baruch G, Fishman A, Menczer J, Struewing JP, et al. Parity, oral contraceptives, and the risk of ovarian cancer among carriers and noncarriers of a BRCA1 or BRCA2 mutation. *N Engl J Med*. 2001;345(4):235–240.
41. Wu NY, Huang HS, Chao TH, Chou HM, Fang C, Qin CZ, Lin CY, Chu TY, Zhou HH. Progesterone prevents high-grade serous ovarian cancer by inducing necroptosis of p53-defective fallopian tube epithelial cells. *Cell Rep*. 2017;18(11): 2557–2565.
42. Wu N, Zhang X, Wang Z, Zhang X, Fang C, Li H, Zhu M, Wang Y, Liao Q, Chu T-Y. Progesterone prevents HGSOC by promoting precancerous cell pyroptosis via inducing fibroblast paracrine. *iScience*. 2023;26(4):106523.
43. Lahiguera Á, Hyroššová P, Figueras A, Garzón D, Moreno R, Soto-Cerrato V, McNeish I, Serra V, Lazaro C, Barretina P, et al. Tumors defective in homologous recombination rely on oxidative metabolism: Relevance to treatments with PARP inhibitors. *EMBO Mol Med*. 2020;12(6):Article e11217.
44. Krishnakumar R, Kraus WL. The PARP side of the nucleus: Molecular actions, physiological outcomes, and clinical targets. *Mol Cell*. 2010;39(1):8–24.
45. Dragos SM, Bergeron KF, Desmarais F, Suitor K, Wright DC, Mounier C, Mutch DM. Reduced SCD1 activity alters markers of fatty acid reesterification, glyceroneogenesis, and lipolysis in murine white adipose tissue and 3T3-L1 adipocytes. *Am J Physiol Cell Physiol*. 2017;313(3):C295–C304.
46. Zou Y, Wang YN, Ma H, He ZH, Tang Y, Guo L, Liu Y, Ding M, Qian SW, Tang QQ. SCD1 promotes lipid mobilization in subcutaneous white adipose tissue. *J Lipid Res*. 2020;61(12):1589–1604.
47. Shimano H, Sato R. SREBP-regulated lipid metabolism: Convergent physiology - divergent pathophysiology. *Nat Rev Endocrinol*. 2017;13(12):710–730.
48. Hassannia B, Vandenabeele P, Vanden Berghe T. Targeting ferroptosis to iron out cancer. *Cancer Cell*. 2019;35(6):830–849.
49. Zhong C, Yang J, Zhang Y, Fan X, Fan Y, Hua N, Li D, Jin S, Li Y, Chen P, et al. TRPM2 mediates hepatic ischemia-reperfusion injury via Ca^{2+}-induced mitochondrial lipid peroxidation through increasing ALOX12 expression. *Research*. 2023;6:0159.
50. Gan B. Mitochondrial regulation of ferroptosis. *J Cell Biol*. 2021;220(9):e202105043.
51. Shaw TJ, Senterman MK, Dawson K, Crane CA, Vanderhyden BC. Characterization of intraperitoneal, orthotopic, and metastatic xenograft models of human ovarian cancer. *Mol Ther*. 2004;10(6):1032–1042.

52. Domcke S, Sinha R, Levine DA, Sander C, Schultz N. Evaluating cell lines as tumour models by comparison of genomic profiles. *Nat Commun*. 2013;4:2126.
53. Beaufort CM, Helmijr JCA, Piskorz AM, Hoogstraat M, Ruigrok-Ritstier K, Besselink N, Murtaza M, van IJcken WFJ, Heine AAJ, Smid M, et al. Ovarian cancer cell line panel (OCCP): Clinical importance of in vitro morphological subtypes. *PLOS ONE*. 2014;9(9):Article e103988.
54. Segaloff A, Weed JC, Parson W. Progesterone therapy of uterine fibromyomas. *J Clin Endocrinol Metab*. 1946;6(10):699.
55. Barton M, Wiesner BP. Thermogenic effect of progesterone. *Lancet*. 1945;2(6380):671.
56. Hoffman MM. Studies in the metabolism of progesterone. *Can Med Assoc J*. 1942;47(5):424–432.
57. Wu NY, Fang C, Huang HS, Wang J, Chu TY. Natural history of ovarian high-grade serous carcinoma from time effects of ovulation inhibition and progesterone clearance of p53-defective lesions. *Mod Pathol*. 2020;33(1):29–37.
58. McCann KE, Hurvitz SA. Advances in the use of PARP inhibitor therapy for breast cancer. *Drugs Context*. 2018;7:212540.
59. Maiorano MFP, Maiorano BA, Biancofiore A, Cormio G, Maiello E. Niraparib and advanced ovarian cancer: A beacon in the non-BRCA mutated setting. *Pharmaceuticals*. 2023;16(9):1261.
60. Murai J, Huang SYN, das BB, Renaud A, Zhang Y, Doroshow JH, Ji J, Takeda S, Pommier Y. Trapping of PARP1 and PARP2 by clinical PARP inhibitors. *Cancer Res*. 2012;72(21):5588–5599.
61. Chen X, Kang R, Kroemer G, Tang D. Broadening horizons: The role of ferroptosis in cancer. *Nat Rev Clin Oncol*. 2021;18(5):280–296.
62. Lei G, Zhuang L, Gan B. Targeting ferroptosis as a vulnerability in cancer. *Nat Rev Cancer*. 2022;22(7):381–396.
63. Mou Y, Wang J, Wu J, He D, Zhang C, Duan C, Li B. Ferroptosis, a new form of cell death: Opportunities and challenges in cancer. *J Hematol Oncol*. 2019;12(1):34.
64. Konstantinopoulos PA, Ceccaldi R, Shapiro GI, D'Andrea AD. Homologous recombination deficiency: Exploiting the fundamental vulnerability of ovarian cancer. *Cancer Discov*. 2015;5(11):1137–1154.
65. Yang W, Yue H, Lu G, Wang W, Deng Y, Ma G, Wei W. Advances in delivering oxidative modulators for disease therapy. *Research*. 2022;2022:9897464.
66. Mei J, Tian H, Huang HS, Hsu CF, Liou Y, Wu N, Zhang W, Chu TY. Cellular models of development of ovarian high-grade serous carcinoma: A review of cell of origin and mechanisms of carcinogenesis. *Cell Prolif*. 2021;54(5):Article e13029.
67. Anglesio MS, Wiegand KC, Melnyk N, Chow C, Salamanca C, Prentice LM, Senz J, Yang W, Spillman MA, Cochrane DR, et al. Type-specific cell line models for type-specific ovarian cancer research. *PLOS ONE*. 2013;8(9):Article e72162.
68. Meng J, Peng J, Feng J, Maurer J, Li X, Li Y, Yao S, Chu R, Pan X, Li J, et al. Niraparib exhibits a synergistic anti-tumor effect with PD-L1 blockade by inducing an immune response in ovarian cancer. *J Transl Med*. 2021;19(1):415.
69. Bizzaro F, Fuso Nerini I, Taylor MA, Anastasia A, Russo M, Damia G, Guffanti F, Guana F, Ostano P, Minoli L, et al. VEGF pathway inhibition potentiates PARP inhibitor efficacy in ovarian cancer independent of BRCA status. *J Hematol Oncol*. 2021;14(1):186.